Polyhedron 30 (2011) 2922–2932

Contents lists available at SciVerse ScienceDirect

Polyhedron

journal homepage: www.elsevier.com/locate/poly

Synthesis, structure studies and electrochemistry of molybdenum(VI) Schiff base complexes in the presence of different donor solvent molecules

Ngui Khiong Ngan *, Kong Mun Lo, Chee Seng Richard Wong

Department of Chemistry, University of Malaya, 50603 Kuala Lumpur, Malaysia

ARTICLE INFO

Article history:
Received 5 August 2011
Accepted 26 August 2011
Available online 10 September 2011

Keywords:
Dioxomolybdenum(VI) complex
Schiff base
Crystal structure

ABSTRACT

The reactions between bis(acetylacetonato)dioxomolybdenum(VI) and Schiff base ligands derived from 5-chlorosalicylaldehyde or 3-ethoxy-salicylaldehye, and 3-methoxy-benzoic hydrazide (*m*-anisic hydrazide), 2-furoic hydrazide or 2,4-dihydroxy-benzoic hydrazide in the presence of donor solvents yielded *cis*-dioxomolybdenum(VI) complexes with the general formula **$MoO_2L(D)$**, where **L** = tridentate Schiff base ligand and **D** = dimethylsulfoxide, hexamethylphosphoramide, dimethylformamide, imidazole or methanol. The complexes were characterized by elemental analysis, electronic spectra, IR, ^1H and ^{13}C NMR spectroscopies, thermogravimetric analysis, cyclic voltammetry, and the molecular structures of five of the dioxomolybdenum complexes were elucidated by single crystal X-ray diffractometion studies. In general, the complexes adopt an octahedral environment around the Mo center with a *cis*-oxo configuration. The other coordination sites are occupied by the imino nitrogen, phenoxyl oxygen, hydroxyl oxygen of the tridentate Schiff base and the donor atom of the solvent molecule. The structural data revealed that the labile coordination site, which is occupied by N or O atoms from the donor solvents, has a longer Mo–O or Mo–N bond distance.

1. Introduction

Molybdenum(VI) and (V) ions normally form complexes containing two terminal oxygen atoms which demonstrate two type of orientations, *cis*-dioxo and *trans*-dioxo [1,2]. A flurry of literature regarding molybdenum(VI) complexes with *cis*-directed terminal oxygen atoms has been presented, but the latter class of compounds is less explored. On the contrary, the *cis*-dioxo compounds display catalytic activities [3]. Since 1978, there has been ample bidentate, tridentate and tetradentate Schiff base ligands reported [4]. The coordination chemistry of molybdenum has been taken cognizance of by the scientific community in the last 20 years due to its ability to access multiple common oxidation state, cycling between +4 and +6, as well as being able to form stable complexes with *N,O* or/and *S* donor atoms ligands [5–15].

The coordination chemistry of molybdenum(VI) with Schiff base ligands has come into the limelight for the synthetic chemist due to its biological activities and catalytic properties. From a biological activity point of view, it has been shown that high valent oxomolybdenum(VI) complexes are effective for redox molybdoenzymatic reactions in living systems [16]. Examples of coordinatively unsaturated molybdenum containing enzymes are sulfite oxidase, which is used in the catalytic conversion of SO_3^{2-} to SO_4^{2-}, and xanthine oxidase which is used in the catalytic conversion of xanthine to uric acid [17]. As a result, several attempts have been made to create a model systems for the active side of molybdo-enzymes [18–21].

In the context of catalytic properties, numerous monomeric dioxomolybdenum complexes have played important roles in many important industry processes, such as oxidation of alcohols and epoxidation of olefins, either in homogenous or heterogenous process [22–24]. Epoxidation is one of the typical reactions in organic synthesis as modification of the intermediate epoxides can produce various synthetic products such as enantioselective drugs, pesticides, epoxy paints, rubber promoters and dyestuffs. Thus, Mo(VI) is an important catalyst precursor for epoxidation reactions [25–27].

Dibasic tridentate ligands together with two terminal oxygen atoms normally form five-coordinate complexes when reacting with the molybdenum(VI) moiety, but the molybdenum ion usually completes its customary sixth coordination site by adopting a solvent molecule or through dimerization (either bridged through one complexing ligand or through the metal center). In the present work, the Schiff base ligands are obtained by the condensation of 5-chloro-salicylaldehyde or 3-ethoxy-salicylaldehyde with *m*-anisic hydrazide, 2-furoic hydrazide or 2,4-dihydroxy-benzoic hydrazide. These tridentate ligands were used for complexation as the complexes formed leave a labile coordination site that can be used for substrate binding. We used several reagents such as DMSO, HMPA, DMF and imidazole to complete the "open"

* Corresponding author.
E-mail address: nicky_ngan@hotmail.com (N.K. Ngan).

0277-5387/$ - see front matter © 2011 Elsevier Ltd. All rights reserved.
doi:10.1016/j.poly.2011.08.038

coordination site in order to investigate the effect of different monodentate donor molecules at the sixth coordination site to the overall structure of the complexes formed. In 1989, Syamal and Maurya reported dioxomolybdenum(VI) complexes with tridentate dibasic Schiff bases derived from various hydrazides, including 2-furoic acid hydrazide [28], but no crystal structures were reported. Since dioxomolybdenum(VI) complexes with –*ONO* donor tridentate Schiff base ligands have been found useful for oxo-transfer reactions, we describe here the synthesis, spectroscopic and electrochemical properties and structures of these complexes.

2. Experimental

2.1. General procedures

All the reagents and solvents used in the synthesis were procured commercially and used without subsequent purification. The starting material, bis(acetylacetonato) dioxomolybdenum(VI), $[MoO_2(acac)_2]$ was prepared as described in the literatures [29,30].

^1H and ^{13}C NMR spectra were measured in DMSO-d_6 on JEOL Lambda and ECA 400 MHz NMR spectrometers. IR spectra were recorded as Nujol mulls in the range 4000–400 cm^{-1} using a Perkin–Elmer 2000 FT-IR instrument. Elemental analysis was performed at the in-house microanalytical laboratory using a Perkin–Elmer 2400 Series II CHNS/O System. Electronic absorption spectral measurement of the ligands and complexes in DMF were measured using a Shimadzu-1650-PC-UV–vis spectrophotometer. Thermal analysis (TGA) of the complexes was carried out by heating in nitrogen gas at a rate of 20 °C per minute on a Perkin Elmer TGA-4000 thermo balance.

Cyclic voltammetry was carried out using a Methrohm Autolab B.V. model. The measurements were done in DMF solution containing 0.1 M TEAP as the supporting electrolyte and a 5×10^{-4} M complex solution, deoxygenated by bubbling with nitrogen gas. The working, counter and reference electrodes used were Pt wire, platinum coil and SCE, respectively.

The X-ray crystallographic intensity data were measured using Mo Kα radiation (graphite crystal monochromator, $\lambda = 0.71069$ Å). The data collection was collected at 296 K on a Bruker APEX II with a CCD area-detector X-ray diffractometer. The structures were solved by direct method with the SHELXS97 program [31] and refined on F^2 by full-matrix least-squares methods with anisotropic non-hydrogen atoms. Crystal data are given in Table 1 and selected bond distances and angles are reported in Table 2.

2.2. Preparation of the ligands

All the Schiff base ligands **L1**, **L2**, **L3** and **L4** were prepared by the condensation reactions of 5-chlorosalicylaldehyde or 3-ethoxylsalicylaldehyde with *m*-anisic hydrazide, 2-furoic hydrazide or 2,4-dihydroxy-benzoic hydrazide in a 1:1 ratio. A typical preparation of the ligands is described as follow:

2.2.1. 5-Chlorosalicylaldehyde 3-methoxy-benzo hydrazone (*L1*)

0.156 g (1.0 mmol) of 5 chlorosalicylaldehyde in 20 ml methanol was added to 20 ml of 0.166 g (1.0 mmol) of *m*-anisic hydrazide. The solution mixture was refluxed with vigorous stirring for 2 h and the color of the solution changed from colorless to yellow. The solution was then allowed to stand at room temperature for 2 days. The bright yellow precipitate was filtered and washed with methanol and dried in air. M.p.: 136 °C; Yield 0.25 g, 82%; *Anal.* Calc. for $C_{15}ClH_{13}N_2O_3$: C, 59.02; H, 4.26; N, 9.18. Found: C, 60.11; H, 4.02; N, 9.21%; IR (KBr) (ν_{max}/cm^{-1}): 3429 ν(m, OH), 1644 ν(s, C=O), 1590 ν(m, C=N), 1566 ν(m, C_{ar}–O), 1278 ν(m, C_{enolic}–O); ^1H NMR (DMSO-d_6, δ ppm): 3.74, (3H, O–CH_3), 6.93–7.40 (aromatic), 8.43 (1H, HC=N), 9.32 (–OH), 11.10 (1H, N–NH); ^{13}C NMR (DMSO-d_6, δ ppm): 159.25 (C=N), 162.71 (C=O), 55.37 (O–CH_3); 110.43, 112.89, 117.78, 118.69, 119.88, 121.32, 129.74, 130.41, 133.59, 134.10, 145.71, 156.42 (aromatic).

Similar procedures were applicable to the preparations of **L2**, **L3** and **L4**.

2.2.2. 5-Chlorosalicylaldehyde-furan-1-carbohydrazone (*L2*)

M.p.: 156 °C; Yield 0.17 g, 65%; *Anal.* Calc. for $C_{12}ClH_9N_2O_3$: C, 54.34; H, 3.40; N, 18.11. Found: C, 53.21; H, 4.02; N, 18.00%; IR (KBr) (ν_{max}/cm^{-1}): 3400 ν(s, N–H), 3134 ν(s, O–H), 1649 ν(s, C=O), 1601 ν(s, C=N), 1267 ν(s, C_{enolic}–O); ^1H NMR (DMSO-d_6, δ ppm): 8.50 (1H, HC=N), 6.67–7.93 (aromatic), 11.07 (1H, N–NH), 12.15 (–OH); ^{13}C NMR (DMSO-d_6, δ ppm): 154.63 (C=N), 156.44 (C=O); 112.72, 115.91, 118.73, 121.34, 123.54, 127.84, 131.31, 146.13, 146.70 (aromatic and furyl ring).

2.2.3. 5-Chlorosalicylaldehyde 2,4 dihydroxy-benzo hydrazone (*L3*)

M.p.: 175 °C; Yield 0.19 g, 71%; *Anal.* Calc. for $C_{14}ClH_{11}N_2O_4$: C, 56.57; H, 3.70; N, 21.89. Found: C, 56.66; H, 4.15; N, 20.91%; IR (KBr) (ν_{max}/cm^{-1}): 3419, 3378, 3162 ν(s, O–H), 1650 ν(s, C=O), 1608 ν(s, C=N), 1514 ν(m, C_{ar}–O); ^1H NMR (DMSO-d_6, δ ppm): 6.31–7.80 (aromatic), 8.60 (1H, HC=N), 11.95 (1H, N–NH), 10.28, 11.26, 12.19, (3 –OH); ^{13}C NMR (DMSO-d_6, δ ppm): 162.93 (C=N), 165.27 (C=O); 102.84, 105.89, 107.60, 118.24, 120.64, 122.96, 127.60, 129.81, 130.80, 145.93, 156.02, 162.22 (aromatic).

2.2.4. 3-Ethoxy-salicylaldehyde 3-methoxy-benzo hydrazone (*L4*)

M.p.: 160 °C; Yield 0.22 g, 69%; *Anal.* Calc. for $C_{16}H_{18}N_2O_4$, 64.97; H, 5.73; N, 8.92. Found: C, 64.33; H, 5.85; N, 8.91%; IR (KBr) (ν_{max}/cm^{-1}): 3424 ν(m, OH), 1652 ν(s, C=O), 1607 ν(m, C=N), 1517 ν(m, C_{ar}–O)); ^1H NMR (DMSO-d_6, δ ppm): 8.64 (1H, HC=N), 6.60–7.50 (aromatic), 10.96, (–OH), 12.05 (1H, N–NH); ^{13}C NMR (DMSO-d_6, δ ppm): 159.28 (C=N), 162.56 (C=O); 112.86, 115.26, 117.75, 118.97, 119.06, 119.85, 121.04, 129.76, 134.21, 147.08, 147.52, 148.41 (aromatic).

2.3. Preparation of the Mo(VI) complexes

A general procedure for the preparation of the Mo(VI) complexes is to reflux a mixture of $MoO_2(acac)_2$ and the ligand in a 1:1 ratio in methanol. A few drops of dimethylsulfoxide (DMSO), hexamethylphosphoramide (HMPA), dimethylformamide (DMF) or a stoichiometric amount of imidazole (Imz) were introduced into the solution, except for the preparation of **C9**. A typical preparation description is given below:

2.3.1. (5-Chlorosalicylaldehyde 3-methoxy-benzylhydrazonato) dimethylsulfoxide dioxomolybdenum(VI) (*C1*)

0.328 g (1.0 mmol) of $MoO_2(acac)_2$ in 20 ml of methanol was mixed with 20 ml of 0.156 g (1.0 mmol) of 5-chlorosalicylaldehyde *m*-anisic hydrazide, after which, a few drops of DMSO were added dropwise until the resulting orange precipitate dissolved completely. The solution mixture was then refluxed with vigorous stirring for 3 h. After leaving the solution for 2 days at room temperature, fine orange crystals were formed. The product was filtered and washed with methanol. M.p.: 196 °C; Yield 0.22 g, 43%; *Anal.* Calc. for $C_{17}ClH_{17}N_2O_6SMo$: C, 40.13; H, 3.34; N, 5.51; S, 6.63. Found: C, 39.59; H, 3.82; N, 5.33; S, 6.57%; IR (KBr) (ν_{max}/cm^{-1}): 1618 (m, C=N), 1523 (m, C=C), 1330 (s, C–O), 1264 (m, C_{enolic}–O), 1033 (m, S–O), 923, 901 (s, Mo=O); ^1H NMR (DMSO-d_6, δ ppm): 3.81 (3H, O–CH_3), 6.93–7.80 (aromatic), 8.89 (1H, HC=N); ^{13}C NMR (DMSO-d_6, δ ppm): 55.36 (O–CH_3), 134.30 (C=N), 169.14 (C=O), 112.60, 118.38, 120.56, 120.61, 121.70, 124.92, 130.14, 131.68, 132.90, 134.30, 155.14 (aromatic).

Table 1
Crystallographic data and structure refinement parameters for compounds **C1**, **C2**, **C3**, **C7** and **C8**.

Compounds	**C1**	**C2**	**C3**	**C7**	**C8**
Chemical formula	$C_{17}H_{17}O_6N_2ClSMo$	$C_{14}H_{13}O_6N_2ClSMo$	$C_{16}H_{16}O_7N_2ClSMo$	$C_{20}H_{23}O_7N_3Mo$	$C_{20}H_{20}O_6N_4Mo$
M_r	509.60	468.71	512.76	513.35	523.09
Crystal color, habit	orange, block	orange, block	red, block	orange, block	orange, block
Crystal size (mm)	0.30 × 0.20 × 0.20	0.30 × 0.20 × 0.20	0.40 × 0.30 × 0.20	0.32 × 0.30 × 0.30	0.35 × 0.30 × 0.20
Crystal system	triclinic	triclinic	monoclinic	triclinic	triclinic
Space group	$P\bar{1}$	$P\bar{1}$	*P2(1)/n*	$P\bar{1}$	$P\bar{1}$
Unit cell dimension					
a (Å)	8.3916(8)	8.2850(1)	10.4049(3)	8.1339(3)	8.8210(1)
b (Å)	11.211(1)	10.0410(2)	14.0625(5)	10.5258(4)	9.641(2)
c (Å)	11.627(1)	10.4913(2)	12.6463(4)	12.9452(6)	12.9167(2)
α (°)	67.539(1)	76.630(1)	90	85.077(2)	84.418(1)
β (°)	81.441(1)	86.463(1)	100.837(2)	72.828(2)	84.627(1)
γ (°)	85.219(1)	87.725(1)	90	88.216(2)	71.938(1)
V (Å^3)	999.2(2)	847.23(3)	1817.2(1)	1064.98(7)	1033.51(3)
Z	2	2	4	2	2
T (K)	100(1)	100(1)	100(1)	100(1)	100(1)
D_{calc} (g cm^{-3})	1.691	1.837	1.867	1.565	1.572
μ (MoKα) (mm^{-1})	0.931	1.089	1.030	0.669	0.581
Absorption correction	multiscan	multiscan	multiscan	multiscan	multiscan
T_{min}	0.7676	0.7359	0.6833	0.7860	0.7996
T_{max}	0.8357	0.8116	0.8204	0.7980	0.8780
F(000)	512	468	1048	524	531
Total data	10368	7878	13092	10571	8701
Unique data	9905	3864	3357	5176	4020
R_{int}	0.0202	0.0136	0.017	0.0187	0.0232
Observed data [$I > 2\sigma(I)$]	3338	3599	8075	4953	3861
Ranges of *h*, *k*, *l*	−9, 9; −13, 13; −13, 13	−10, 10; −13, 13; −13, 13	−12, 12; −17, 17; −15, 15	−10, 10; −14, 14; −17, 17	−11, 11; −12, 12; −17, 17
Number of parameter	256	228	257	284	272
R_1	0.0258	0.0260	0.0396	0.0255	0.0262
wR_2	0.0754	0.0690	0.0731	0.0807	0.0713
S	1.087	1.090	1.138	1.022	1.116
$\Delta\rho_{max}$ (e Å^{-3})	0.813	0.925	1.043	0.590	0.770
$\Delta\rho_{min}$ (e Å^{-3})	−0.582	−0.714	−1.172	−1.203	−0.469

Table 2
Selected bond distances (Å) and bond angles (°) for **C1**, **C2**, **C3**, **C7** and **C8**.

	C1	**C2**	**C3**	**C7**	**C8**
Bond distance					
Mo(1)–O(1)	1.9313(17)	1.9374(16)	1.933(2)	1.9240(14)	1.9437(17)
Mo(1)–O(2)	1.6996(19)	1.7113(16)	1.711(3)	1.7088(14)	1.7069(16)
Mo(1)–O(3)	1.698(2)	1.6972(17)	1.691(3)	1.7032(15)	1.7069(17)
Mo(1)–O(4)	1.9949(16)	2.0101(17)	2.009(2)	2.0216(13)	2.0136(16)
Mo(1)–N(1)	2.2565(19)	2.2436(19)	2.242(3)	2.2295(16)	2.2474(19)
Mo(1)–O(6)/N(3)	2.2808(17)	2.2660(16)	2.336(3)	2.2958(15)	2.351(2)
C(8)/(10)–N(2)	1.300(3)	1.300(3)	1.303(5)	1.298(3)	1.298(3)
C(8)/(10)–O(4)	1.326(3)	1.330(3)	1.327(4)	1.324(2)	1.326(3)
C(1)–O(1)	1.343(3)	1.349 (3)	1.347(4)	1.335(2)	1.349(3)
N(1)–N(2)	1.400(3)	1.393(3)	1.392(4)	1.400(2)	1.393(3)
C(7)/(9)–N(1)	1.280(3)	1.290(3)	1.284(5)	1.284(3)	1.291(3)
Bond angle					
O(2)–Mo(1)–O(3)	105.12(11)	104.67(8)	104.14(13)	105.40(7)	105.46(8)
O(3)–Mo(1)–O(1)	98.57(9)	97.73(8)	99.05(12)	98.96(7)	97.00(8)
O(2)–Mo(1)–O(1)	103.75(8)	104.62(7)	104.56(11)	105.07(6)	105.04(7)
O(3)–Mo(1)–O(4)	98.14(9)	98.22(8)	97.42(12)	96.44(6)	97.93(7)
O(2)–Mo(1)–O(4)	96.70(8)	95.68(7)	97.46(11)	94.11(6)	96.81(7)
O(1)–Mo(1)–O(4)	149.10(7)	149.99(7)	148.22(10)	151.10(6)	149.09(7)
O(3)–Mo(1)–N(1)	91.76(9)	92.63(8)	90.63(12)	95.37(7)	89.92(8)
O(2)–Mo(1)–N(1)	160.77(9)	160.19(8)	163.11(12)	156.25(7)	162.12(8)
O(1)–Mo(1)–N(1)	82.29(7)	82.07(7)	80.66(11)	82.47(6)	81.51(7)
O(4)–Mo(1)–N(1)	71.39(7)	71.96(7)	72.15(10)	71.83(6)	71.61(6)
O(3)–Mo(1)–O(6)/N(3)	168.11(9)	169.16(7)	176.34(11)	169.58(6)	170.71(7)
O(2)–Mo(1)–O(6)/N(3)	86.77(9)	86.07(7)	79.38(11)	84.98(6)	83.82(8)
O(1)–Mo(1)–O(6)/N(3)	77.90(7)	77.76(7)	80.89(10)	78.79(6)	79.94(7)
O(4)–Mo(1)–O(6)/N(3)	80.43(7)	81.90(6)	80.99(10)	81.65(6)	81.00(7)
O(6)/N(3)–Mo(1)–N(1)	76.56(7)	77.05(6)	85.74(10)	74.30(6)	80.97(7)

A similar procedure to that above was used to prepare the following complexes:

*2.3.2. (5-Chlorosalicylaldehyde furan-1-carbohydrazonato) dimethylsulfoxide dioxomolybdenum(VI) (**C2**)*

M.p.: 320 °C; Yield 0.11 g, 23.45%; *Anal.* Calc. for $C_{14}ClH_{13}N_2O_6SMo$: C, 35.78; H, 2.98; N, 5.96; S, 6.82. Found: C, 36.39; H, 2.41; N, 6.38; S, 6.84%; IR (KBr) (ν_{max}/cm^{-1}): 1625 (m, C=N), 1521 (w, C=C), 1260 (m, C_{enolic}–O), 1095 (m, S–O), 925, 903 (s, Mo=O); ^1H NMR (DMSO-d_6, δ ppm): 6.69–7.93 (aromatic and furyl ring), 8.85 (1H, HC=N); ^{13}C NMR (DMSO-d_6, δ ppm): 158.48 (C=N), 162.44 (C=O), 113.14, 117.05, 121.06, 122.19, 125.45, 133.30, 134.62, 144.90, 147.61, 155.20, 158.48 (aromatic and furoic ring).

*2.3.3. (5-Chlorosalicylaldehyde 2,4 dihydroxy-benzohydrazonato) dimethylsulfoxide dioxomolybdenum(VI) (**C3**)*

M.p.: 300 °C; Yield 0.13 g, 25%; *Anal.* Calc. for $C_{16}ClH_{16}N_2O_7SMo$: C, 37.54; H, 3.13; O, 21.90; N, 5.47; S, 6.26. Found: C, 37.82; H, 2.77; N, 5.81; S, 5.81%; IR (KBr) (ν_{max}/cm^{-1}): 3172 (OH), 1627 (s, C=N), 1546 (m, C_{ar}–O), 1513 (m, C=C), 1262 (m, C_{enolic}–O), 1095 (s, S–O), 927, 907 (s, Mo=O); ^1H NMR (DMSO-d_6, δ ppm): 6.30–7.74 (aromatic), 8.91 (1H, HC=N), 11.33 and 10.32 (2 –OH); ^{13}C NMR (DMSO-d_6, δ ppm): 55.36 (O–CH_3), 163.56 (C=N), 170.08 (C=O), 102.91, 104.89, 108.72, 120.80, 121.86, 125.26, 131.14, 134.28, 153.57, 158.01, 161.00 (aromatic).

*2.3.4. (5-Chlorosalicylaldehyde furan-1-carbohydrazonato) hexamethylphosphoramide dioxomolybdenum(VI) dimethylformamide solvate (**C4**)*

0.328 g (1.0 mmol) of $MoO_2(acac)_2$ in 20 ml of methanol was mixed with 20 ml of 0.156 g (1.0 mmol) of 5-chlorosalicylaldehyde *m*-anisic hydrazide, after which, a few drops of HMPA were added and an orange precipitate was obtained. DMF was added dropwise until the precipitate dissolved completely. The solution mixture was then refluxed with vigorous stirring for 3 h. The solution was left for 2 days at room temperature to obtain fine orange crystals. The product was filtered and washed with methanol. M.p.: 131 °C; Yield 0.13 g, 22%; *Anal.* Calc. for $C_{18}ClH_{26}O_6N_5PMo$: C, 38.08; H, 4.54; N, 12.22. Found: C, 37.71; H, 4.47; N, 12.93%; IR (KBr) (ν_{max}/cm^{-1}): 1681, 1624 (m, C=N), 1515 (w, $C_{phenolic}$–O), 1343 (m, C–O), 1268 (m, C_{enolic}–O), 1157 (s, P=O), 930, 906 (s, Mo=O); ^1H NMR ($CDCl_3$, δ ppm): 2.50 (18H, HMPA), 2.85 and 2.94 (DMF), 7.06–8.01 (aromatic and furyl ring), 8.41 (1H, HC=N); ^{13}C NMR ($CDCl_3$, δ ppm): 36.72 and 36.68 (HMPA), 162.88 (C=N), 163.14 (C=O), 31.64 (DMF), 112.06, 116.17, 120.76, 121.73, 125.42, 132.00, 133.69, 145.62, 145.42, 152.68, 158.92 (aromatic and furoic ring).

A similar procedure to that above was used to prepare the following complexes:

*2.3.5. (3-Ethoxysalicylaldehyde 3-methoxy-benzohydrazonato) hexamethylphosphoramide dioxomolybdenum(VI) (**C5**)*

M.p.: 124 °C; Yield 0.09 g, 17%; *Anal.* Calc. for $C_{23}H_{36}N_5O_7PMo$: C, 44.45; H, 5.84; N, 11.27. Found C, 45.21; H, 6.10; N, 11.37%; IR (KBr) (ν_{max}/cm^{-1}): 1618 (s, C=N), 1606 (m, C=C), 1566 (m, C_{ar}–O), 1257 (m, C_{enolic}–O), 1150 (s, P=O), 929, 903 (Mo=O); ^1H NMR (DMSO-d_6, δ ppm): 2.50 and 2.52 (HMPA) 3.85, (3H, O–CH_3), 4.08 (5H, O–C_2H_5), 6.93–7.80 (aromatic), 8.49 (1H, HC=N); ^{13}C NMR (DMSO d_6, δ ppm): 36.56, 36.60 (HMPA), 65.60 (O–C_2H_5), 159.44 (C=N), 170.06 (C=O), 112.75, 118.00, 119.58, 120.45, 121.06, 121.28, 125.45, 129.19, 132.54, 148.63, 151.49, 153.82 (12C, aromatic).

*2.3.6. (3-Ethoxysalicylaldehyde-3-methoxy-benzolhydrazonato) dimethylsulfoxide dioxomolybdenum(VI) (**C6**)*

M.p.: 184 °C; Yield 0.17 g, 30%; *Anal.* Calc. for $C_{19}H_{24}N_2O_7SMo$: C, 43.85; H, 4.62; N, 5.38; S, 6.15. Found: C, 44.59; H, 4.22; N, 5.74; S, 6.24%; IR (KBr) (ν_{max}/cm^{-1}): 1618 (s, C=N), 1596 (m, C=C), 1564 (m, C_{ar}–O), 1257 (m, C_{enolic}–O), 1082 (s, S–O), 925, 894 (Mo=O); ^1H NMR (DMSO-d_6, δ ppm): 3.78, (3H, O–CH_3), 4.04 (5H,O–C_2H_5), 6.97–7.54 (aromatic), 8.91 (1H, HC=N); ^{13}C NMR (DMSO-d_6, δ ppm): 55.81 (O–CH_3), 55.81 (O–CH_3), 64.85 (O–C_2H_5), 159.88 (C=N), 169.02 (C=O), 112.91, 120.92, 121.22, 122.08, 126.06, 130.55, 148.02, 149.84, 156.75 (12C, aromatic).

*2.3.7. (3-Ethoxysalicylaldehyde 3-methoxy-benzohydrazonato) dimethylformamide dioxomolybdenum(VI) (**C7**)*

M.p.: 118 °C; Yield 0.10 g, 19%; *Anal.* Calc. for $C_{20}H_{23}N_3O_7Mo$: C, 46.78; H, 4.48; N, 8.17. Found: C, 46.87; H, 4.41; N; 8.02%; IR (KBr) (ν_{max}/cm^{-1}): 1616 (s, C=N), 1597 (m, C=C), 1565 (m, C_{ar}–O), 1258 (m, C_{enolic}–O), 725 (s, NC=O_{DMF}), 931, 906 (Mo=O); ^1H NMR (DMSO-d_6, δ ppm): 2.89 and 2.73 (DMF), 7.01–7.95 (aromatic), 8.94 (1H, HC=N); ^{13}C NMR (DMSO-d_6, δ ppm): 30.76 and 35.77 (DMF), 159.30 (C=N), 162.31 (C=O), 112.42, 118.12, 120.37, 121.52, 125.55, 130.00, 147.60, 156.19 (aromatic ring).

*2.3.8. (3-Ethoxysalicylaldehyde 3-methoxy-benzohydrazonato) imidazole dioxomolybdenum(VI)methanol solvate (**C8**)*

M.p.: 235 °C; Yield 0.14 g, 27%; *Anal.* Calc. for $C_{20}H_{20}N_4O_6Mo$: C, 46.97; H, 4.11; N, 10.96. Found: C, 46.78; H, 4.36; N; 10.57%; IR (KBr) (ν_{max}/cm^{-1}): 1596 (s, C=C), 1561 (m, C_{ar}–O), 1258 (m, C_{enolic}–O), 3133 (m), 1067 (w, N–H_{Imz}), 922, 903 (s, Mo=O); ^1H NMR (DMSO-d_6, δ ppm): 6.95 (m, Imz), 7.18–7.53 (aromatic), 8.88 (1H, HC=N); ^{13}C NMR (DMSO-d_6, δ ppm): 159.83 (C=N), 169.07 (C=O), 121.22, 130.55 and 131.87 (Imz), 112.91, 118.68, 119.13, 120.22, 122.08, 126.06, 148.12, 149.95, 156.75 (aromatic ring).

*2.3.9. (3-Ethoxysalicylaldehyde 3-methoxy-benzylhydrazonato) methanol dioxomolybdenum(VI) (**C9**)*

M.p.: 140 °C; Yield 0.25 g, 55%; *Anal.* Calc. for $C_{18}H_{20}N_2O_7M_1$: C, 45.76; H, 4.24; N, 5.93. Found: C, 45.89; H, 4.12; N, 5.79%; IR (KBr) (ν_{max}/cm^{-1}): 1608 (s, C=N), 1562 (m, C_{ar}–O), 1260 (m, C_{enolic}–O), 3430 (w, C–$O_{methanol}$), 949, 921 (s, Mo=O); ^1H NMR (DMSO-d_6, δ ppm): 1.34 (CH_3–O*H*), 3.80 (*CH*$_3$–OH), 6.97–7.58 (aromatic), 8.93 (1H, HC=N); ^{13}C NMR (DMSO, δ ppm): 159.30 (C=N), 168.54 (C=O), 112.42, 118.11, 118.68, 120.37, 120.70, 121.52, 125.56, 130.00, 131.36, 147.61, 149.47, 156.19 (aromatic).

3. Results and discussion

3.1. Synthesis

The synthesized ligands were reacted with bis(acetylacetonato) dioxomolybdenum(VI) in methanol solution under refluxing conditions. However, the reaction mixture produced a sandy precipitate, with poor yields. However, when DMSO, DMF, HMPA or imidazole was introduced into the reaction mixture, fine crystalline complexes of the general formula **$MoO_2L(D)$**, (D = DMSO, HMPA, DMF, imidazole) were obtained, as shown in Scheme 1. This indicates that DMSO, DMF, HMPA and imidazole are stronger donor solvents compared to methanol. In the case of **C4**, DMF was added during the preparation of the complex due to the low solubility of the complex in methanol. The preliminary crystal structure of **C4** revealed that HMPA is directly attached to the MoO_2^{2+} core instead of DMF. From the crystallographic data, **C4** has a rather short Mo–O(6) bond distance, compared to that of **C7**. This implicates that HMPA coordinates well to the MoO_2^{2+} core. The ONO donor types of Schiff base ligands show keto-enol tautomerization both in solution and in

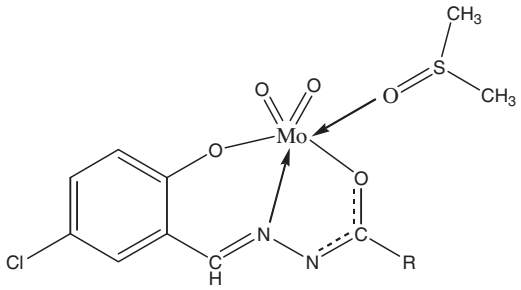

R=3-(CH₃O)C₆H₄ (**C1**), *2-C₄H₃O* (**C2**), *2,4-(OH)₂C₆H₃* (**C3**)

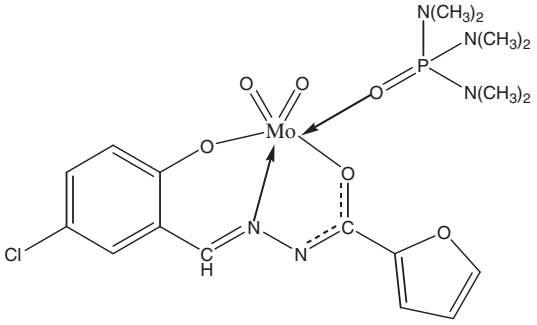

C4

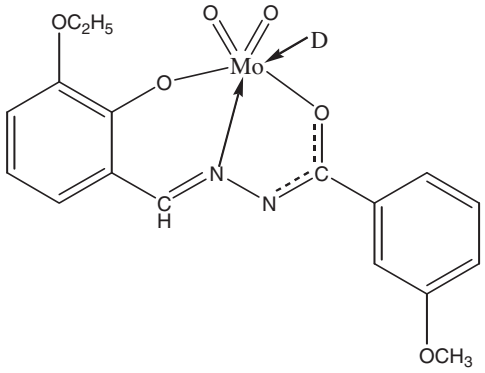

D: HMPA (**C5**), *DMSO* (**C6**), *DMF* (**C7**), *Imz* (**C8**), *Methanol* (**C9**)

Scheme 1. Dioxomolybdenum(VI) complexes with dibasic tridentate Schiff base ligands in the presence of different donor solvent molecules.

the solid state. The delocalized bond in the enolate group has given rise to a slight difference in the elemental analysis results. In general, the six coordinated Mo(VI) complexes readily undergo a facial displacement reaction at the sixth coordination site. This is corroborated by the TGA study, which exhibited the initial lose of the donor solvent molecules on controlled heating. The products obtained ranged from red to orange, and are air stable in the solid state. The complexes are sparingly soluble in chloroform and ethanol, except **C4**, but highly soluble in DMSO and DMF.

3.2. IR and NMR spectroscopic description

The IR spectra of all the complexes **C1**–**C9** reveal two absorption bands in the region 890–930 cm^{-1}, which is attributed to the vibration of the two double-bonded *cis*-oxygen atoms at the molybdenum core [32,33]. The sixth coordination site of the complexes is occupied by the solvent molecules, which gives rise to an octahedral geometry at the molybdenum center. The spectra of **C1**, **C2**, **C3** and **C6** were found to contain absorption bands in the range 1030–1095 cm^{-1} which are due to the ν(S–O) stretching. In the case of **C4** and **C5**, the bands at 1157 and 1150 cm^{-1} are associated with ν(P–O) stretching. The stretching frequencies of NC=O of DMF and N–H of imidazole in the complexes **C7** and **C8** were at 725 and 1067 cm^{-1}, respectively [34]. The shift to lower frequency for the functional groups –S=O, –C=O and –P=O, compared to the free ligands, indicate that Mo(VI) attached to DMSO, DMF, HMPA and imidazole through the oxygen or nitrogen atom.

The IR spectra of **L1** and **L2** exhibit a few ligand bands, $\nu_{(OH)}$ at 3136 and 3156 cm^{-1}, $\nu_{(NH)}$ at 3386 cm^{-1} and $\nu_{(C=O)}$ at 1650 cm^{-1}. Upon coordinating to MoO_2^{2+}, these absorption bands disappear, as shown in the spectra of complexes **C1–C9** [7]. In the case of complex **C3**, an absorption band at 3172 cm^{-1}, attributed to the –OH stretching of the 2,4-dihydroxy-benzoic hydrazide, was clearly observed. The characteristic –C=N– imine band in **L1** and **L2**, which exists at 1588 and 1590 cm^{-1}, was found to have shifted to higher frequency in **C1**–**C9** [5]. The $\nu(C_{ar}–O)$ band in the range 1520–1540 cm^{-1} for the ligands was found to have shifted to the higher frequency of 1560 ± 5 cm^{-1}, suggesting the coordination of the deprotonated phenolic C–O group to the MoO_2 moiety. Likewise, the presence of a new band at 1255 ± 5 cm^{-1} in the complexes could be assignable to $\nu(C_{enolic}–O)$.

The ^{1}H NMR spectra of **L1** and **L2** exhibit a $–OH_{phenolic}$ proton resonance at δ 9.32 and 12.15 ppm and a $H_{imine}–C=N$ resonance at δ 8.43 and 8.58 ppm, respectively. Upon coordination to the Mo atom, the –OH signal disappeared, which is due to the deprotonation of $OH_{phenolic}$ and the coordination of the oxygen atom to the Mo atom. The participation of the imine nitrogen in complexation is signaled by an appreciable downfield shift of the azomethine proton signal (δ 8.89 and 8.85 for **C1** and **C2**, respectively). The presence of MeOH (**C9**), imidazole (**C8**), DMF (**C7**) and HMPA (**C5**) in the complexes is shown by resonance peaks at δ 3.38, 121–131, 2.89 and 2.73, and 2.50, respectively.

3.3. Crystallographic description of the complexes

The molecular structures of **C1**, **C2**, **C3**, **C7** and **C8** (Figs. 1–5) show that in all of the complexes the Schiff base ligands behave as tridentate ligands, and have reacted with the dioxomolybdenum anion to form six coordinated molybdenum(VI) structures. As shown in the figures, the imine nitrogen, one of the phenoxyl oxygens and the hydroxyl oxygen from the enolized carbonyl group are involved in the coordination with molybdenum atom, forming six- and five-member chelate rings around the *cis*-MoO_2 center. The overall geometry can be regarded as an octahedron, with the equatorial plane formed by the imine nitrogen, phenoxyl oxygen, hydroxyl oxygen and one of the terminal oxygen atoms of the dioxomolybdenum unit. The other terminal oxygen and the donor atom from the solvent occupy the apical positions.

In all of the complexes, the Mo=O bond lengths which range from 1.693(2) to 1.721(2) Å and the O=Mo=O bond angles, which

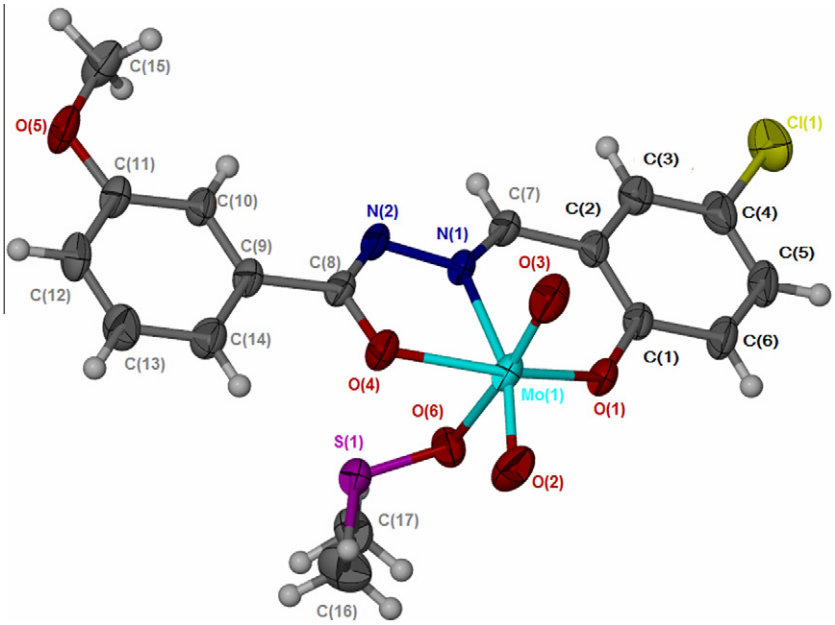

Fig. 1. ORTEP plot of $MoO_2L1(DMSO)$, **C1**, with the atom labeling scheme.

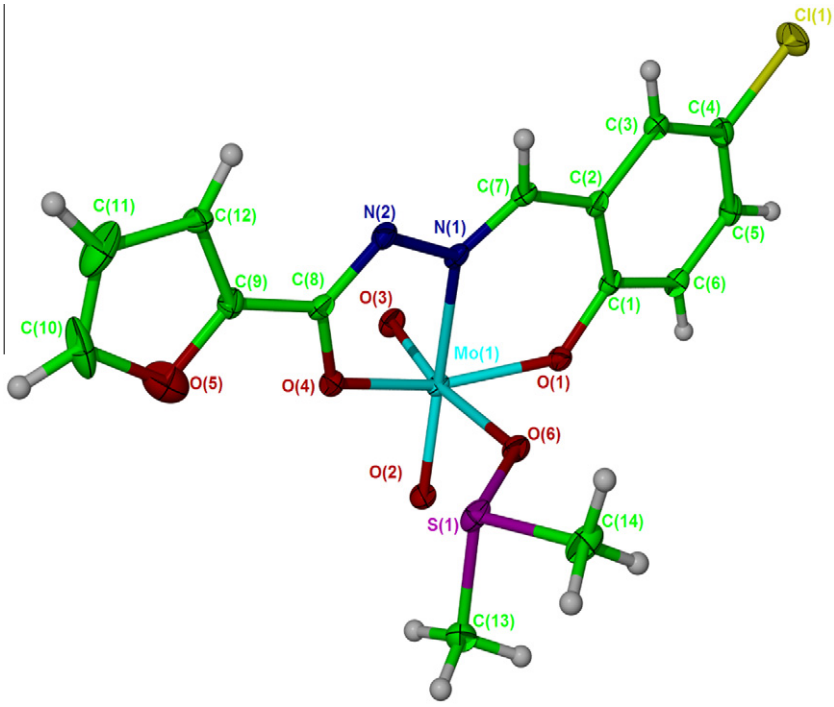

Fig. 2. ORTEP plot of $MoO_2L2(DMS)$, **C2**, with the atom labeling scheme.

lie between 104.23(2)° and 105.40(2)°, are similar to those reported for other MoO_2 complexes [35–38]. The bond distances between the Mo atom and the phenolate oxygen, deprotonated nitrogen and the enolate oxygen atoms are also close to those found in other ONO tridentate Schiff base molybdenum(VI) complexes. The C–O bond distance in all the complexes exhibit values between 1.309 and 1.326 Å, which is nearer to a C–O single bond than to a C–O double bond distance. This shows that the ligand coordinates to the MoO_2 core in the deprotonated enolate form [8–10].

The Mo–O (donor atom of solvent) bond length in the molecular structures of **C1**, **C2**, **C3**, **C7** and **C8** are all somewhat longer than the normal single bond length due to the consequence of the *trans* effect of M = O_t (where O_t is the oxo-group *trans* to the Mo–$O_{solvent}$ bond). This result reveals a rather weak attachment of the solvent donor atom to MoO_2^{2+}. When the methanol coordinated MoO_2(VI) complexes are dissolved in stronger coordinating agents, such as DMF, DMSO or HMPA, the methanol molecule tends to be displaced by these solvent molecules.

The equatorial bases formed by O1, O2, O4 and N1 in the complexes are not coplanar. The Mo atom in molecular structures of **C1** and **C8** are found to have shifted 0.2010 and 0.2233 Å, respectively, out from the basal plane towards the apical oxo-oxygen atom O3,

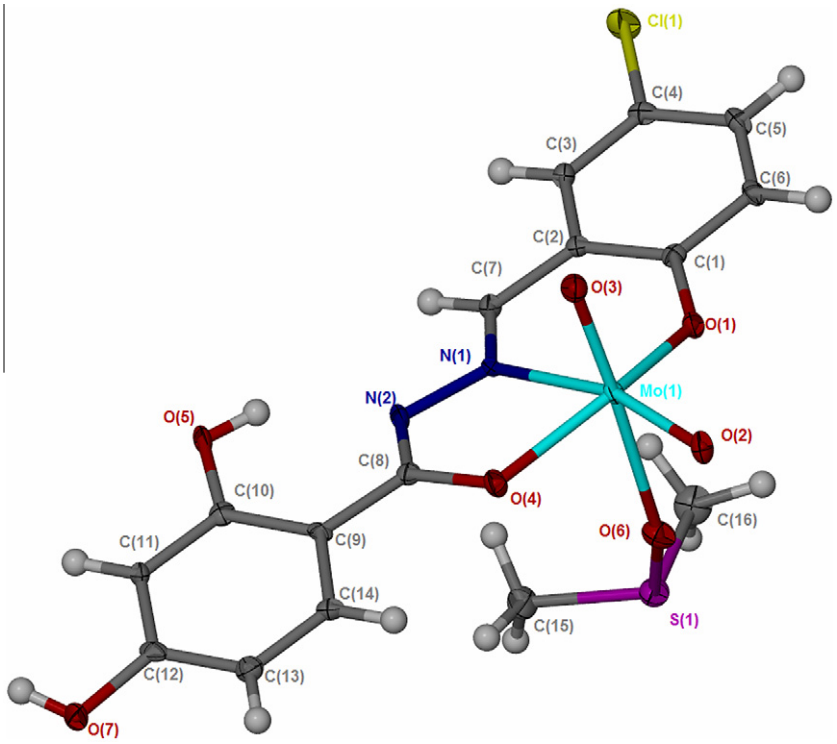

Fig. 3. ORTEP plot of $MoO_2L3(DMSO)$ **C3**, with the atom labeling scheme.

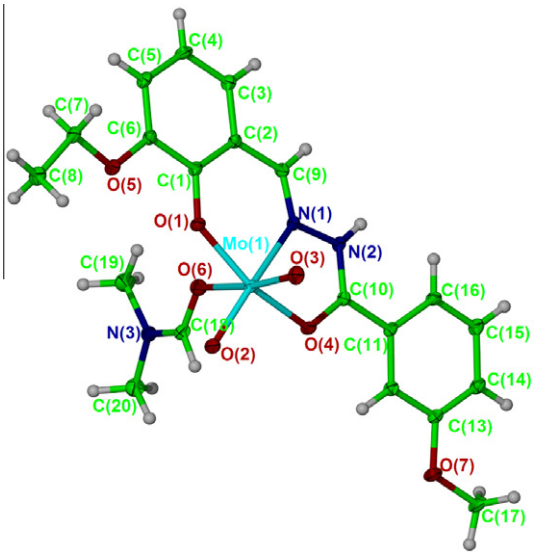

Fig. 4. ORTEP plot of $MoO_2L4(DMF)$ **C7**, with the atom labeling scheme.

while the other structures show a displacement of the metal atom towards the donor atom of the solvent, O6.

In the molecular structure of **C3** (Fig. 6), intramolecular O–H···N hydrogen bonding (2.602(4) Å) in the Schiff base ligand helps to stabilize the overall structure. In addition, the presence of OH···O hydrogen bonding (O7H···O2, 2.826(4) Å and O7H···O6, 3.069(4) Å) links the molecules into a polymeric chain parallel to the *ab* crystallographic plane (Table 3). The unusual Mo1–O6 bond length (2.337 Å) and the O6–Mo1–O2 angle (176.18°) are the consequence of the hydrogen bonding interactions of the **C3** molecules. In the crystal structure of **C8** (Fig. 7), the presence of a methanol molecule which is hydrogen bonded to the imidazole nitrogen (N–H···O, 2.864(6) Å) results in a layer structure propagating along the *bc* crystallographic plane (Table 4). The π–π contacts between the imidazole rings, *Cg1*–*Cg1′* (symmetry code: $1-x, 1-y, 1-z$, where *Cg1* is the centroid of the imidazole ring), may further stabilize the structure, with a centroid–centroid distance of 3.813(2) Å. On the other hand, complexes **C1**, **C2** and **C7** exist as discrete molecules with no evidence of any hydrogen bonding interactions.

3.4. Thermal properties

The thermogravimetric analysis of the complexes was carried out in the temperature range 50–900 °C at a heating rate of 20 °C min^{-1}. All the complexes are stable until 150 °C, except for **C1** and **C9**, in which weight losses of 3.51% and 7.00% were observed that could be due to the removal of water and methanol molecules in the compounds. Above this temperature, the TG curves show three steps of weigh losses. The first step of decomposition in the temperature range 150–250 °C involved the removal of solvent molecules (DMSO, DMF, HMPA or imidazole). With further elevation in temperature, a rapid weigh loss in the temperature range 250–370 °C followed by a gradual weigh loss in the temperature range 370–700 °C was observed. The total decomposition of the second and third stage weight losses may be ascribed to the dissociation of the Schiff base ligand at the –C=N– bond before it is removed from the Mo^{2+} core. Decomposition continues until the final residue, MoO_2, is left. Thermal decomposition data of the complexes are given in Table 5. The TG curve for the selected complexes **C1** and **C5** are shown in Fig. 8. In general, the thermal decomposition behavior of the complexes can be summarized in Scheme 2.

3.5. Electronic spectra

Electronic absorption bands of the ligands and complexes in 5×10^{-4} M DMF are given in Table 6. For the ligands, two absorp-

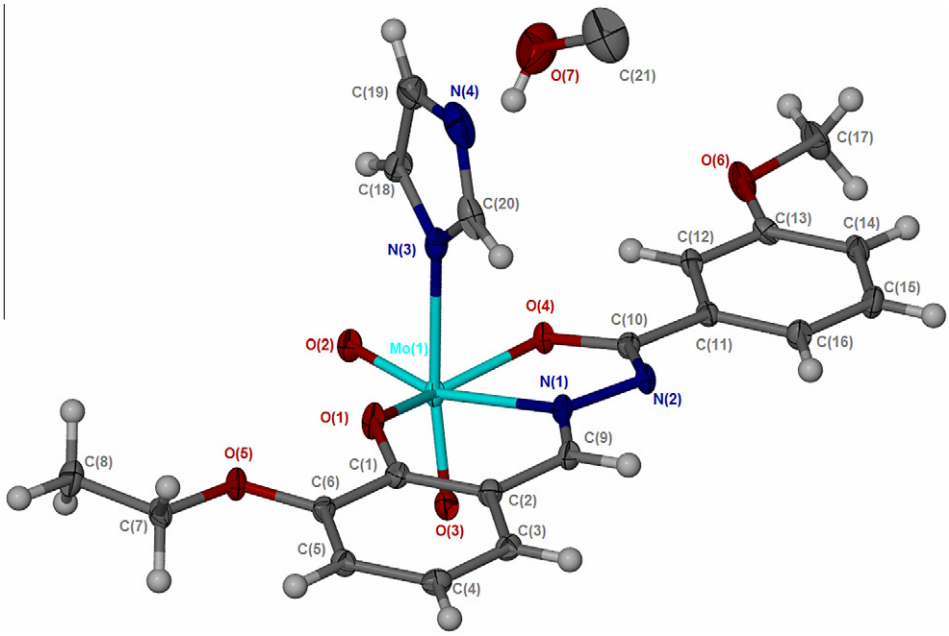

Fig. 5. ORTEP plot of $MoO_2L4(Imz)$ **C8**, with the atom labeling scheme.

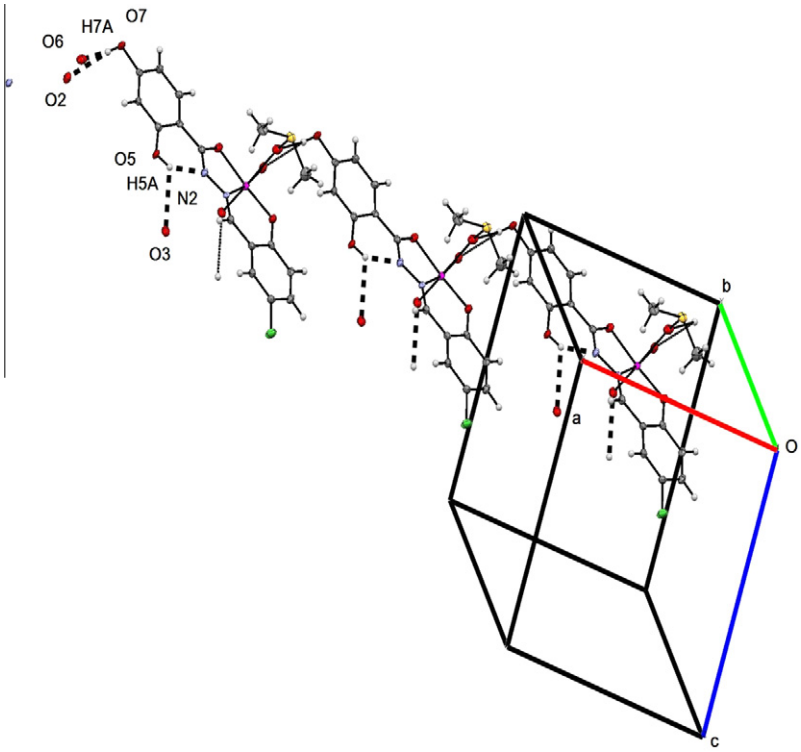

Fig. 6. Intra- and intermolecular hydrogen bonds in the crystal structure of **C3**.

Table 3
Hydrogen bonds for **C3** [Å and °].

D–H···A	*d*(D–H)	*d*(H···A)	*d*(D···A)	∠(DHA)
O(5)–H(5A)···N(2)	0.82	1.89	2.601(4)	144.7
O(5)–H(5A)···O(3)#1	0.82	2.55	3.075(4)	123.5
O(7)–H(7A)···O(2)#2	0.82	2.20	2.826(4)	133.0
O(7)–H(7A)···O(6)#2	0.82	2.30	3.069(4)	155.6

Symmetry transformations used to generate equivalent atoms: #1: $-x+1$, $-y+2$, $-z+1$; #2: $x+1$, y, z.

tion bands observed at *ca.* 292 and 302 nm are probably due to *n* to π^* transitions of the –C═N– and –C═O– moieties of the ligands [39]. The absorption band at *ca.* 338 nm may be assigned to *n* to π^* transitions of the aromatic rings. The spectra of the complexes show a broad band at 400–410 nm, which is assignable to a ligand to metal charge transfer (LMCT) due to the promotion of an electron from the highest occupied molecular orbital (HOMO) of the ligand to the lowest unoccupied molecular orbital (LUMO) of molybdenum atom [40]. Other LMCT bands, which are observable

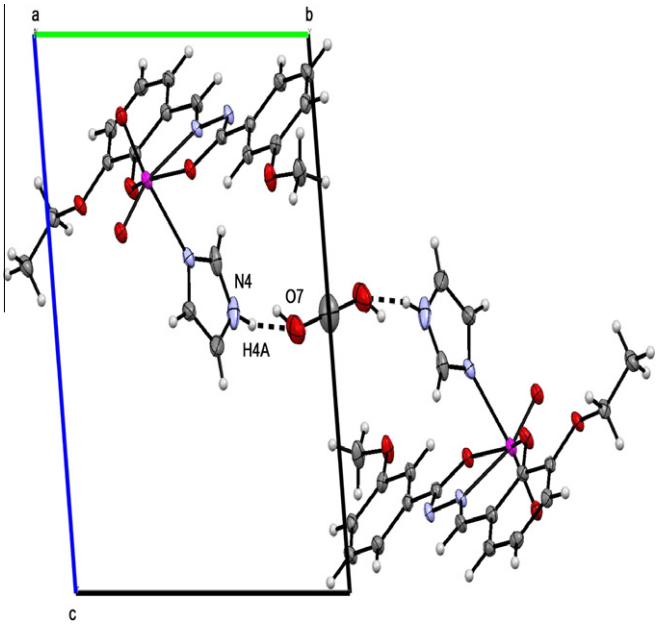

Fig. 7. C8 molecules are linked by N–H···O hydrogen bonds.

Table 4
Hydrogen bonds for **C8** [Å and °].

D–H···A	*d*(D–H)	*d*(H···A)	*d*(D···A)	∠(DHA)
N(4)–H(4A)···O(7)	0.86	2.02	2.862(5)	165.4

Symmetry transformations used to generate equivalent atoms: #1: $-x+1$, $-y+2$, $-z+1$.

around 290 and 350 nm, can be ascribed to the oxygen to molybdenum and nitrogen to the molybdenum charge transfer transitions, respectively. Higher energy bands appearing below 290 nm are due to intra-ligand transitions. The absence of a *d*–*d* transition absorption band in the visible region confirms the $4d^0$ electronic configuration of Mo(VI) [41].

3.6. Electrochemical studies

The redox behavior of the ligands and the complexes were examined in DMF solution using cyclic voltammetry at a platinum electrode with 0.1 M tetraethyl ammonium perchlorate (TEAP) as the supporting electrolyte. The CV data is tabulated and selected I versus E profiles are illustrated in Fig. 9. From the data, **L1**, **L2** and **L4** exhibit an irreversible one oxidative peak around −0.55 V, while **L3** shows reversible electrochemical behavior. For a completely reversible one-electron transfer reaction independent of scan rate, a ΔE = 58 mV and a ratio of 1 for the anodic and cathodic peak currents are obtainable. For these complexes, one oxidative and reductive response are scrutinized near to −0.80 and −1.10 V, respectively. The oxidation wave in the complexes is due to the effect of the redox behavior of the ligands, as the observed values fall in the same region as that for the free ligands. Only the reduction wave in the complexes is attributable to a reduction at the molybdenum centers. Reduction of **C1** and **C2** occured at 0.96 and 0.84 V. In the case of **L3** and **C3**, both oxidative and reductive responses appeared approximately in the same region. However, in the case of **C5**–**C9**, the cathodic reduction potentials occur around −1.17 V. The more negative the cathodic reduction potential, the more difficult it is for the dioxomolybdenum(VI) complexes to be reduced. Both the electron donating groups ($-OC_2H_5$) and the additional aromatic ring for greater electron delocalization in **L4** are probably the leading contributors to the shift to more negative values of the cathodic reduction potential in **C5**–**C9** [42–44]. In general, CV studies on these *cis*-dioxomolybdenum(VI) complexes revealed irreversible redox behavior.

4. Conclusion

Several mononuclear dioxomolybdenum(VI) complexes with different donor solvent molecules have been synthesized and characterized by various physicochemical techniques and by X-ray

Table 5
Thermogravimetric Analysis of the complexes.

Compounds	Temp. range (°C)	Weight loss observed (calculated) (%)	Molecules removed	End residue
C1	(a) 50–100	(a) 3.51 (3.41)	(a) H_2O[a]	MoO_2
	(b) 150–270	(b) 15.24 (14.77)	(b) DMSO	
	(c) 270–370	(c) 31.68 (30.87)	(c) $-NNCOC_6H_4OCH_3$	
	(d) 370–650	(d) 25.66 (26.52)	(d) $-OC_7H_5Cl$	
C2	(a) 170–280	(a) 15.66 (16.60)	(a) DMSO	MoO_2
	(b) 280–340	(b) 30.07 (29.57)	(b) $-NNCOC_4H_3O$	
	(c) 340–700	(c) 26.33 (26.17)	(c) $-OC_7H_5Cl$	
C3	(a) 180–260	(a) 14.92 (15.24)	(a) DMSO	MoO_2
	(b) 260–370	(b) 20.84 (21.28)	(b) $-C_6H_4(OH)_2$	
	(c) 370–760	(c) 37.00 (37.30)	(c) $-ClC_6H_4CNNCO$	
C4	(a) 150–300	(a) 42.31 (40.62)	(a) HMPA + DMF	MoO_2
	(b) 300–850	(b) 39.14 (40.40)	(b) $ClC_6H_3OCN_2COC_4H_3O$	
C5	(a) 170–300	(a) 52.63 (55.53)	(a) HMPA + $-N_2COC_6H_4OCH_3$	MoO_2
	(b) 300–850	(b) 22.23 (22.80)	(b) $-OC_2H_5C_6H_3OC$	
C6	(a) 190–280	(a) 13.92 (15.34)	(a) DMSO	MoO_2
	(b) 280–300	(b) 27.06 (29.00)	(b) $-OC_2H_5C_6H_3OC$	
	(c) 300–750	(c) 30.11 (32.08)	(c) $-NNCOC_6H_4OCH_3$	
C7	(a) 160–250	(a) 13.60 (14.20)	(a) DMF	MoO_2
	(b) 250–330	(b) 32.00 (31.71)	(b) $-NNCOC_6H_4OCH_3$	
	(c) 330–700	(c) 30.09 (28.27)	(c) $-OC_2H_5C_6H_3OC$	
C8	(a) 170–310	(a) 46.36 (44.68)	(a) Imidazole + $CH_3OH-NNCOC_6H_4OCH_3$	MoO_2
	(b) 310–700	(b) 30.66 (28.54)	(b) $-OC_2H_5C_6H_3OC$	
C9	(a) 70–110	(a) 7.00 (6.79)	(a) CH_3OH	MoO_2
	(b) 110–320	(b) 35.00 (34.39)	(b) $-NNCOC_6H_4OCH_3$	
	(c) 320–700	(c) 30.77 (31.42)	(c) $-OC_2H_5C_6H_3OC$	

[a] Water molecules come from the air moisture and this is corroborated by elemental analysis.

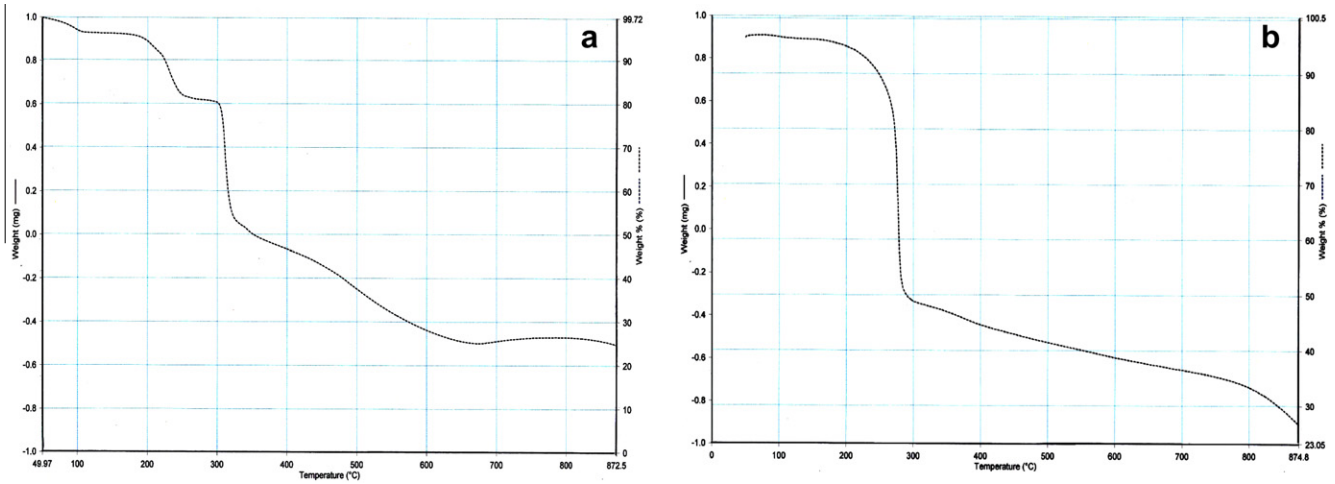

Fig. 8. (a) Thermogram for **C1** and (b) thermogram for **C5**.

$$MoO_2(ONO')D \xrightarrow[150\text{-}270^oC]{-D} MoO_2(ONO') \xrightarrow[250\text{-}370^oC]{-NO'} MoO_2(O) \xrightarrow[370\text{-}700^oC]{-O} MoO_2$$

D : Solvent molecules

ONO' : Tridentate ligands

Scheme 2. Thermal decomposition of the dioxomolybdenum(VI) complexes.

Table 6
Electronic spectra band position and cyclic voltammetry data.

Compounds	λ_{max} (nm)	E_p/V (vs. SCE)
L1	338, 302, 291	−0.58
L2	338, 303, 292	−0.51
L3	339, 313, 293, 225	−0.55, −1.08
L4	301, 262	−0.54
C1	409, 336, 304, 292	−0.61, −0.96
C2	409, 314, 268, 227	−0.53, −0.84, −1.11, −1.52
C3	414, 340, 316, 278	−0.75, −1.04
C4	410, 325, 305, 279	−0.49, −0.83, −1.08, −1.46
C5	315, 270, 209	−0.88, −1.18
C6	314, 276, 267	−0.83, −1.17
C7	382, 301	−0.85, −1.17
C8	397, 361, 302	−0.56, −1.17
C9	345, 269	−0.68, −1.15

crystallographic diffraction. TGA analysis and crystallographic data revealed that the donor solvent molecules are attached loosely to the MoO_2^{2+} unit resulting in substitution reactions at the sixth coordination site more easily. This was shown in the case of **C4** and **C8**, in which the sixth coordination site was occupied by HMPA and imidazole, respectively, additionally solvated by DMF and methanol, respectively. On the other hand, the presence of an hydroxyl group as a substituent in the chelating ligands affects the molecular geometry of the complex **C3** through hydrogen bonding interactions. An electrochemical study shows irreversible redox behavior of the *cis*-dioxomolybdenum(VI) complexes.

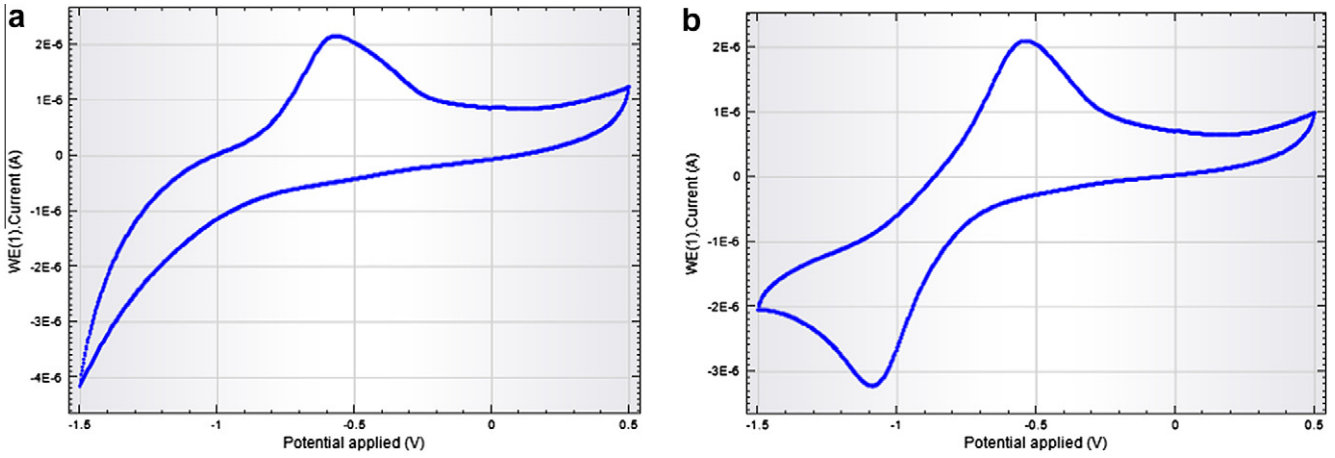

Fig. 9. Cyclic voltammogram for **L1** (a) and **L3** (b) – scan rate 100 mV/s.

Acknowledgement

We wish to thank the University of Malaya (PS378/2010B and RG020/09AFR) for supporting this study.

Appendix A. Supplementary material

CCDC 825060, 825061, 825062, 826698 and 826699 contains the supplementary crystallographic data for this paper. These data can be obtained free of charge via http://www.ccdc.cam.ac.uk/conts/retrieving.html, or from the Cambridge Crystallographic Data Centre, 12 Union Road, Cambridge CB2 1EZ, UK; fax: (+44) 1223 336 033; or e-mail: deposit@ccdc.cam.ac.uk.

References

[1] S.J. Mo, B.K. Koo, Bull. Korean Chem. Soc. 20 (1999) 1105.
[2] V. Mckee, C.J. Wilkin, J. Chem. Soc., Dalton Trans. (1987) 523.
[3] M.H. Chisholm, Inorganic Chemistry: Towards the 21st Century, ACS Symposium Series 211.
[4] W.E. Hill, N. Atabay, C.A. Mc, F.P. Auliffe, Mc. Cullough, S.M. Razzoki, Inorg. Chim. Acta 35 (1979) 35.
[5] K. Yamanouchi, S. Yamada, Inorg. Chim. Acta 9 (1974) 161.
[6] K. Yamanouchi, S. Yamada, J.H. Enemark, Inorg. Chim. Acta 85 (1984) 129.
[7] R. Dinda, P. Sengupta, S. Ghosh, H. Mayer-Figgie, W.S. Sheldrick, J. Chem. Soc., Dalton Trans. (2002) 4434.
[8] C. Zhang, G. Rheinwald, V. Lozan, B. Wu, P.G. Lassahn, H. Lang, C. Janiak, Z. Anorg., Allg. Chem. 628 (2002) 1259.
[9] T. Carofiglio, E. Solari, C. Floriani, Polyhedron 15 (1996) 4435.
[10] S. Duman, I. Kizilcikli, A. Kaca, M. Akkurt, B. Ulkuseven, Polyhedron 29 (2010) 2924.
[11] M. Cindric, N. Strukam, V. Vrdoljak, T. Kajfez, B. Kamenar, Croat. Chem. Acta 76 (2003) 257.
[12] D. Millic, V. Vrdoljak, D. Matkovic-Calogovic, M. Cinddric, J. Chem. Crystallogr. 39 (2009) 553.
[13] Z.D. Tomic, A. Kapor, A. Zmiric, V.M. Leovac, D. Zobel, S.D. Zaric, Inorg. Chim. Acta 360 (2007) 2197.
[14] E.B. Seena, M.R. Prathapachandra Kurup, Polyhedron 26 (2007) 3595.
[15] V. Vrdoljak, M. Cindric, D. Milic, D. Matkovic-Calogovic, Polyhedron 24 (2005) 1717.
[16] R.A.D. Wentworth, Coord. Chem. Rev. 18 (1980) 1.
[17] B.E. Schultz, S.F. Gheller, M.C. Muetterties, M.J. Scott, R.H. Holm, J. Am. Chem. Soc. 115 (1993) 2714.
[18] Jeremy M. Berg, R.H. Holm, J. Am. Chem. Soc. 107 (1985) 917.
[19] Jeremy M. Berg, R.H. Holm, J. Am. Chem. Soc. 107 (1985) 925.
[20] A. Rana, R. Dinda, P. Sengupta, S. Ghosh, L.R. Falvello, Polyhedron 21 (2002) 1023.
[21] J.A. Craig, E.W. Harlan, B.S. Snyder, M.A. Whitener, R.H. Holm, Inorg. Chem. 28 (1989) 2082.
[22] J.M. Bregeault, J. Chem. Soc., Dalton Trans. 1 (2003) 3289.
[23] K.A. Jorgensen, Chem. Rev. 89 (1989) 431.
[24] V.A. Anabela, J. Moreira, A.D. Lopes, M. Pillinger, C.D. Nunes, V.C. Ramao, F.E. Kuhn, I.S. Goncalves, New J. Chem. 28 (2004) 308.
[25] M. Masteri-Parahani, F. Farzaneh, M. Ghandi, J. Mol. Catal. A 192 (2003) 103.
[26] H. Mimoun, G. Wikinson, R.D. Gillard, J.A. McCleverty (Eds.), Compr. Coord. Chem., 6 (1987) 317–339.
[27] F.E. Kuhn, M. Groarke, E. Bencze, E. Herdtweck, A. Prazeres, A.M. Santos, M.J. Calhorda, C.C. Romao, I.S. Goncalves, A.D. Lopes, M. Pillinger, Chem. Eur. J. 8 (2002) 2370.
[28] A. Syamal, M.R. Maurya, Transition Met. Chem. 11 (1986) 235.
[29] D. Loganathan, U. Aich, Glycobiology 16 (2006) 343.
[30] M.M. Jones, J. Am. Chem. Soc. 81 (1959) 3188.
[31] G.M. Shedrick, Acta Cryst. A64 (2008) 112.
[32] P.C.H. Mitchell, Quart. Rev. 20 (1966) 103.
[33] K. Nakamoto, Infrared Spectra of Inorganic and Coordination Compounds, vol. 77, John Wiley, New York, 1963.
[34] A. Bruce, J.L. Curbin, P.L. Dahlstrom, J.R. Hyde, M. Minelli, E.I. Stiefel, J.T. Spence, J. Zubieta, Inorg. Chem. 21 (1982) 917.
[35] C. Bustos, O. Burckhardt, R. Schrebler, D. Carrillo, A.M. Arif, A.H. Cowley, C.M. Nunn, Inorg. Chem. 29 (1990) 3996.
[36] I. Buchan, C.D. Garner, J. Am. Chem. Soc. 106 (1984) 3035.
[37] O.A. Rajan, A. Chakravorty, Inorg. Chem. 20 (1981) 660.
[38] W. Fuller, J. Phys. Chem. 63 (1959) 1705.
[39] L.M. Fostiak, I. Garcia, J.K. Swearingen, E. Bermejo, A. Castineiras, D.X. West, Polyhedron 22 (2003) 83.
[40] J.H. Enemark, C.G. Young, Adv. Inorg. Chem. 40 (1993) 1.
[41] C.S.J. Chang, J.H. Enemark, Inorg. Chem. 30 (1991) 683.
[42] J. Topich, Inorg. Chem. 20 (1981) 3704.
[43] S. Purohit, A. Koley, P. Prasad, P.T. Manoharan, S. Ghosh, Inorg. Chem. 28 (1989) 3735.
[44] S. Gupta, A.K. Barik, S. Pal, A. Hazra, S. Roy, R.J. Butcher, S.K. Kar, Polyhedron 26 (2007) 133.